INTERNATIONAL JOURNAL OF HYDROGEN ENERGY 47 (2022) 6745–6754

Available online at www.sciencedirect.com

ScienceDirect

journal homepage: www.elsevier.com/locate/he

Planar proton-conducting ceramic cells for hydrogen extraction: Mechanical properties, electrochemical performance and up-scaling

Stéven Pirou [a,*], Qingjie Wang [a], Peyman Khajavi [a], Xanthi Georgolamprou [a], Sandrine Ricote [b], Ming Chen [a], Ragnar Kiebach [a]

[a] Department of Energy Conversion and Storage, Technical University of Denmark, Kgs, Lyngby, Denmark
[b] Department of Mechanical Engineering, Colorado School of Mines, Golden, USA

HIGHLIGHTS

- The study showed promising results for large-scale development of efficient PCC[1] cells.
- Microstructural stability of BCZY27[2] based cells were studied.
- BCZY27 based protonic membranes were up-scaled to an area of 135 cm^2.
- The fracture toughness of BCZY27-Ni was studied by double torsion for the first time.
- An electrochemical stability test performed over 400 h showed stable performances.

GRAPHICAL ABSTRACT

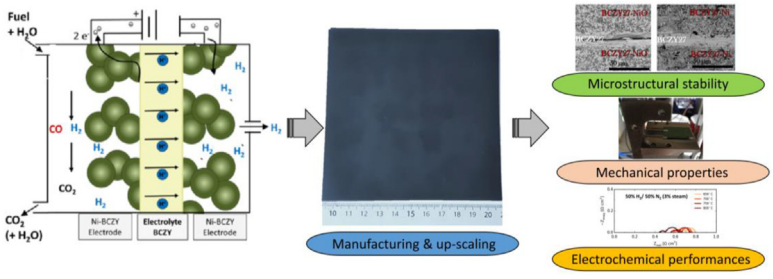

ARTICLE INFO

Article history:
Received 19 August 2021
Received in revised form
13 November 2021
Accepted 5 December 2021
Available online 7 January 2022

Keywords:
Proton-conducting ceramics
Tape-casting

ABSTRACT

Proton-conducting ceramics, which selectively separate H_2 from any hydrogen-containing gas could play a role in the future of the growing hydrogen market. In recent years, membrane technologies related to H_2 extraction became attractive solutions to produce pressurized high-purity hydrogen. Yttrium-doped barium zirconate/cerate materials ($BaCe_xZr_{1-x-y}Y_yO_{3-\delta}$) are among the most studied and used materials. In this study, symmetrical cells consisting of a protonic electrolyte ($BaCe_{0.2}Zr_{0.7}Y_{0.1}O_{3-\delta}$ (BCZY27), 10–15 μm in thickness) surrounded by two cermet electrodes (BCZY27–Ni (50–50 vol%), 150 μm) were prepared for H_2 extraction applications. The cells were prepared via tape-casting and co-sintered at 1575 °C. The cells were up-scaled to an area of 135 cm^2. The fracture toughness of the cermet electrodes was determined to be 2.07 (±0.05) MPa · $m^{1/2}$ at room

* *Corresponding author*. Anker Engelunds Vej, Building 301, 2800 Kgs, Lyngby, Denmark.
E-mail addresses: stepir@dtu.dk (S. Pirou), qinwa@dtu.dk (Q. Wang), pkha@dtu.dk (P. Khajavi), xageor@dtu.dk (X. Georgolamprou), sricote@mines.edu (S. Ricote), minc@dtu.dk (M. Chen), woki@dtu.dk (R. Kiebach).

[1] Proton-conducting ceramics
[2] $BaCe_{0.2}Zr_{0.7}Y_{0.1}O_{3-\delta}$

https://doi.org/10.1016/j.ijhydene.2021.12.041

BCZY
H_2 production
Mechanical properties

temperature using the double torsion technique. Impedance spectra were recorded on the symmetrical cells between 650 and 800 °C in 3% humidified 50% H_2/50% N_2 atmosphere and at 650 °C varying the hydrogen partial pressure (20% < pH_2<100%). In 50% H_2/50% N_2 with 3% H_2O the cells demonstrated an ohmic resistance of 0.59 and 0.44 Ω cm^2, an average electrode polarization resistance of 0.10 and 0.09 Ω cm^2 (per one electrode) at 650 and 800 °C, respectively. Moreover, a stability test was performed over 400 h highlighting the stable electrochemical properties of the symmetrical membranes.

Introduction

Nowadays, hydrogen represents a key resource for several sectors such as the refining industry and the fertilizer industry (e.g. ammonia production), but hydrogen is also expected to play a major role in enabling large-scale efficient renewable energy integration [1]. In this context, membrane technologies related to H_2 extraction became attractive solutions to produce high purity hydrogen (theoretical selectivity of 100%). Proton-conducting ceramics (PCCs), which selectively separate H_2 from any hydrogen-containing gas, can steam reform conventional fuels like gasoline and diesel, and produce hydrogen. Such electrochemical devices could, for example, be used in onboard fuel processors for direct hydrogen extraction from hydrocarbon fuels to enable an increased market share of fuel cell powered vehicles in the next decades [2–4]. The hydrogen extracted from the PCCs can then be electrochemically pumped through proton-exchange membrane fuel cells to power the vehicles.

A PCC is a gas–tight layer permeable only to hydrogen ions (protons), which allows extraction of hydrogen from gas mixtures with a theoretical selectivity of 100%. The majority of the research efforts on the PCC technology has been devoted to Protonic Ceramic Fuel/Electrolysis Cells (PCFC/PCEC), the conversion of methane into aromatics, the dehydrogenation of ethane to ethylene and the production of hydrogen from methane [5–11]. In light of recent progress, PCC can now operate from 300 to 600 °C on a variety of fuels [12–16]. Nevertheless, to limit the bulk resistance related to the transport of hydrogen ions through the PCC, and therefore be more efficient, the proton-conducting layer has to be as thin as possible. Contrary to PCFC operation where one electrode is in oxidizing atmosphere, both electrodes of membranes for hydrogen extraction are in chemically reducing environments. Consequently, symmetrical cells, consisting of a thin dense proton-conducting electrolyte sandwiched between two ceramic-metal (cermet) electrodes, can be applied.

In general, cerate-based protonic conductors exhibit high conductivity but rather poor chemical stability [17]. In contrast, zirconate-based protonic conductors are stable, but their conductivity is limited by highly resistive grain boundaries [18,19]. These results suggest that solid solutions between cerate and zirconate may have both protonic conductivity and good chemical stability. Yttrium-doped barium zirconate/cerate materials ($BaCe_xZr_{1-x-y}Y_yO_{3-\delta}$, BCZY) are among the most studied and used materials for intermediate-temperature proton conductor in PCFCs/PCECs and in hydrogen separation membranes because they exhibit promising protonic conductivity at temperatures of ca. 600 °C [9–11,16,20–24]. Unfortunately, BCZY requires sintering temperatures above 1600 °C to reach relative densities higher than 95% [20,24]. The sintering temperatures can be decreased significantly with the use of sintering aid, such as NiO or ZnO [25–28].

The role of the cermet electrodes is to mechanically support the protonic-conducting layer (electrolyte) and serve as catalyst for hydrocarbon steam reforming thanks to good electronic conductivity. Composites consisting of Ni (electron-conducting catalyst) and ceramic proton conductor (BCZY) have been reported as potential candidates for the cermet electrodes as they show satisfactory electrochemical performance and stability [29–33].

In this study, symmetrical cells consisting of a protonic electrolyte ($BaCe_{0.2}Zr_{0.7}Y_{0.1}O_{3-\delta}$ (BCZY27) + 1 wt% NiO, 10–15 μm) surrounded by two cermet electrodes (BCZY27–Ni (50–50 vol%), 150 μm) were prepared for H_2 extraction applications. BCZY27 was chosen as the electrolyte composition due to a good compromise between thermodynamic stability and low grain boundary resistance. The electrolyte and electrode layers were tape-casted, laminated, and co-sintered at 1575 °C for 6 h. The cells were up-scaled to an area of 135 cm^2. The microstructure of the cells was characterized by Scanning Electron Microscopy (SEM). The formation of significant cracks was observed in the electrolyte after only a few days of storage. A series of experiments were run to understand the cause of the cracks, and a solution was found to solve this challenge. Finally, the fracture toughness of the cermet electrodes and the electrochemical performances of the cells were studied and will be discussed in this paper.

Experimental

Membranes fabrication

The tape casting technology was employed for the preparation of the PCC cells. It is a well-proven technique used to produce thin planar ceramic tapes (generally from 10 μm to a

few millimeters in dry thickness), and also suitable for further scaling-up [34].

The first step of the membrane fabrication comprises the tape casting of (i) the BCZY27–NiO (50–50 vol%) support and (ii) the BCZY27 (+1 wt% NiO, as sintering aid [27]) electrolyte. The BCZY27 and NiO powders were purchased from Marion Technologies (France) and Alfa Aesar (USA), respectively. Suspensions for tape-casting (called slurries) were manufactured by means of ball milling of powders with dispersant (polyvinyl pyrrolidone (PVP)), binder/plasticizer system (polyvinyl butyral (PVB), triethylene glycol di-2-ethylhexanoate, polyethylene glycol, polyoxyethylene aryl ether), and solvent. Powders, dispersant and solvents were ball-milled together to de-agglomerate the powders. Then the binder/plasticizer system was added to the slurries and mixed for an additional 24 h. The suspensions were sieved and de-aired by vacuum treatment before being cast. The support was tape cast on a Mylar foil using a doctor blade gap of 1050 μm, while the electrolyte tape was prepared using a doctor blade gap of 200 μm. Further details on tape preparation can be found here [35].

The next step of the cell fabrication consisted of laminating the above-mentioned support and electrolyte to form a symmetrical structure (support/electrolyte/support). The lamination was performed with heated rolls in a double roll set-up. It was executed at 120 °C in one pass.

The green symmetrical cells were then debinded in air at 600 °C for 4 h using a heating ramp of 15 °C/h, and sintered in air at 1575 °C for 6 h using heating and cooling ramps of 200 °C/h. The laminated tapes shrank around 23% during co-sintering, leading to cell dimensions of 15 cm^2 (3.85 × 3.85 cm^2), and 135 cm^2 (11.6 × 11.6 cm^2), for cells used for the microstructural stability study and the up-scaled cells, respectively. Afterward, the membranes were heat-treated at 900 °C for 10 h in 5% H_2 balanced with N_2 (dry atmosphere) to reduce the NiO to Ni, consequently creating connected porosity in the support layers. Heating and cooling ramps of 120 °C/h were used.

Characterization

Microstructural characterization

To understand the crack formation occurring during storage, the following experimental procedure was performed: first, to discover when the cracks appear in the electrolyte, PCC cells were prepared and analyzed by SEM directly after sintering, after 1, 3, 7, and 10 days of storage in atmospheric conditions in the laboratory and after 10 days of storage under vacuum. The cells stored under vacuum were placed in aluminum bags directly after sintering using a vacuum packaging machine (Jumpo plus, Henkelman, Netherlands). Three cells were analyzed for each storage duration.

Secondly, two thermal treatment options were suggested to solve the challenge of crack formation:

- PCC cells were sintered and immediately reduced in 5% H_2 atmosphere (balanced with N_2). The heat treatment used for reduction of the cells is described Fig. 1a. Three PCC membranes were analyzed by SEM directly after reduction, and after reduction followed by 1, 3, 7, 10, and 120 days of storage in atmospheric conditions and after 10 days of storage under vacuum.
- PCC cells were sintered and heat-treated in moist air containing 1.5% of water. The heat treatment used for hydration of the cells is described Fig. 1b. Three PCC cells were analyzed by SEM directly after hydration, and after hydration followed by 1, 3, 7, and 10 days of storage in atmospheric conditions and after 10 days of storage under vacuum.

The microstructure of the PCC cells was investigated on fractured cross-sections by SEM using a Hitachi TM3000 equipped with a Bruker energy dispersive X-ray spectroscopy (EDX) system. To avoid degrading the microstructure of the cells, the samples were simply fractured and gently polished by hand on silicon carbide grinding papers.

Fracture toughness

Fracture toughness of the BCZY27–Ni support was determined using the Double Torsion (DT) technique in ambient air at room temperature. Rectangular specimens with dimensions of 20 × 40 mm^2 were cut from the sintered and reduced support using laser cutting. A notch with the width and length of 0.5 and 10 mm, respectively, was laser cut on all specimens. In a typical DT experiment, the specimen was placed on four ceramic rollers, and the roller was placed on the notch. The DT experiments were carried out with a displacement rate of 600 μm/min. The plateau loads obtained from the load-displacement curves were then used in the toughness calculations. Further details on the notch geometry, loading configuration, and toughness calculations can be found in Ref. [36]. In total, five specimens were tested. The specimens had a thickness of 290 (±15) μm. The porosity of the specimens was calculated based on their weight, volume, and theoretical density.

Electrochemical impedance spectroscopy

The electrochemical performance and durability of the symmetrical cells were investigated in an in-house built 1-atm testing rig. The cells were mounted to an alumina housing, with fully automated changes of testing conditions (temperatures, gas). The details of the setup for the symmetrical cell measurements can be found in previous work [37–39]. Pt paste was used as the current collector on both electrodes and was sintered in-situ. The cells were heated in 5% H_2 atmosphere (balanced with N_2) to 800 °C with a heating rate of 1 °C/min. Once at temperature, the gas was fed through a water bubbler kept at room temperature, resulting in 3% steam in the gas stream. The electrochemical performance of the cells under various hydrogen partial pressures (20–100%) with 3% steam was evaluated in the temperature range 650–800 °C. Slow cooling and heating ramp rates (60 °C/h) were used to prevent the electrolyte from cracking due to the hydration/dehydration induced chemical expansion. To ensure that the samples were at equilibrium when collecting spectra, a dwell time of 2 h was employed after each change in conditions. The electrochemical performance of the cells was characterized by electrochemical impedance spectroscopy (EIS) using a Solartron 1260 frequency response analyzer at frequencies from 96,485 to 0.06 Hz with an amplitude of 0.33 V. The in-house

developed Python-based software Ravdav was used for plotting and analyzing the EIS data [40].

Results and discussion

Microstructural stability

SEM analyses of symmetrical PCC cells proved that directly after sintering, the microstructure of the electrolyte is intact (see Fig. 2a). Nevertheless, after a few days of storage in atmospheric conditions, similar SEM analyses performed with the same samples revealed cracks in the electrolyte (see Fig. 2d and g). This degradation leading to an extremely short cell lifetime is obviously a serious obstacle for PCC development, which needs to be understood and solved. Based on literature, the formation of cracks in barium zirconate perovskites can be closely related to uncontrolled chemical expansion upon water uptake [41]. This phenomenon happens when proton-conducting materials are exposed to different water vapor conditions. Consequently, stresses grow on the interfaces, which eventually can lead to crack formation.

As described in section: Microstructural characterization., a large number of PCC cells (i.e. 57) were prepared to investigate crack formation observed in the electrolyte and propose a solution to solve this challenge. The experiments can be summarized in three groups.

- the sintered samples,
- the reduced samples (reduction performed immediately after sintering): an assumption was made that the stress grown at the interfaces support/electrolyte led to the cracks and that this stress could be partially removed by reducing the dense BCZY27–NiO support to porous BCZY27–Ni. Moreover, the reduction of NiO in Ni decreases the thermal expansion coefficient (TEC) mismatch between the support layer and the electrolyte.
- the hydrated samples (hydration performed immediately after sintering). Hydration was an attempt to verify if controlled water uptake would lead to a full hydration state that could potentially chemically stabilize the samples and prevent cracks in the electrolyte.

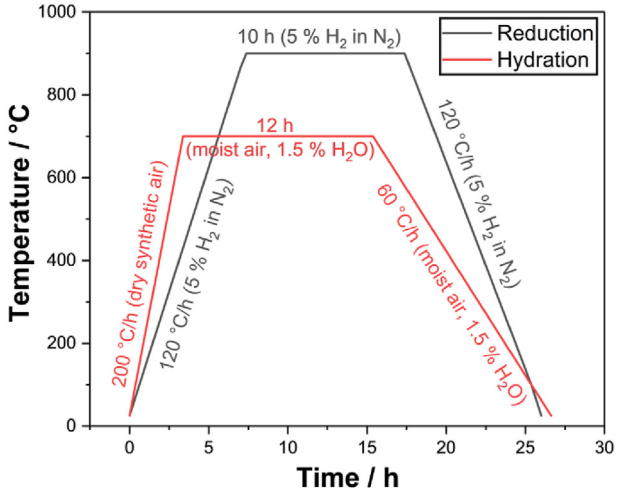

Fig. 1 – Reduction and hydration thermal profiles.

Table 1 summarizes the results of the experiments, where green means that no cracks were observed in any of the three analyzed samples, red signifies that all analyzed samples were cracked, yellow stands for the appearance of cracks in some of the samples, and white/no color indicate that no analysis was performed.

Immediately after the last thermal treatment, the electrolytes of sintered, reduced, and hydrated cells appear dense and crack-free, as shown by the SEM images in Fig. 2a, b, and c. After 1 day of storage in atmospheric conditions, the electrolyte of one of the three sintered samples and all of the hydrated cells was already cracked. The cracks are longitudinal and continuous from one side of the cells to the other. Their positions correspond to the symmetrical axis of the PCC cells, which could indicate that the cracks are due to mechanical stress occurring in the entire surface of the cells. Conversely, the electrolyte of the reduced cells was intact. After 3 days of storage in atmospheric conditions, the tendency is confirmed: all sintered and hydrated cells are cracked (Fig. 2d and f), while all reduced cells are intact (Fig. 2e). The cells analyzed after 10 days of storage corroborate the results, as shown Fig. 2g, h and i. The study also showed that cracking could not be avoided on sintered cells stored in vacuum as after only 10 days PCC cells stored under vacuum were found cracked. Long-term microstructural stability was proven after observing that reduced PCC cells stored for 120 days in atmospheric conditions remain crack-free.

The challenge of microstructural stability being solved, focus was put on up-scaling. Protonic cells up to 135 cm^2 (11.6 × 11.6 cm^2) were successfully produced as shown in Fig. 3. The cells are flat and without apparent defects. The depletion of NiO on the first 1–5 μm of the cells, leading to a dense BCZY skin on the surfaces is the only minor issue observed on the cells. This problem can be easily fixed by slightly polishing the surfaces of the cells or by using NiO powder beds during sintering. The development of industrial-size symmetrical BCZY27 cells represents an encouraging result in the field of hydrogen permeation membranes.

Fracture toughness of the BCZY27–Ni support

Thanks to their high mechanical properties, yttria-stabilized zirconia-based ceramics are commonly used as mechanical supports, e.g. in solid oxide fuel and electrolysis cells (SOCs) and membranes [42–45]. The state-of-the-art (SoA) fuel electrode support in SOCs is made of 3 mol% yttria-stabilized zirconia (3YSZ)–NiO composite, which once reduced forms 3YSZ–Ni cermet [46,47]. In this study, we compared the average fracture toughness value of BCZY27–Ni with that of the SoA 3YSZ-Ni (at porosity of ≈29% and measured under similar conditions, i.e. temperature, atmosphere, and loading rate) [36]. The results are presented in Fig. 4. The calculated Ni contents of the BCZY27–Ni and 3YSZ–Ni supports are ≈37 and 40 vol%, respectively.

As seen, the average fracture toughness of the BCZY27–Ni samples correspond to 2.07 (SD 0.05) MPa $m^{1/2}$,

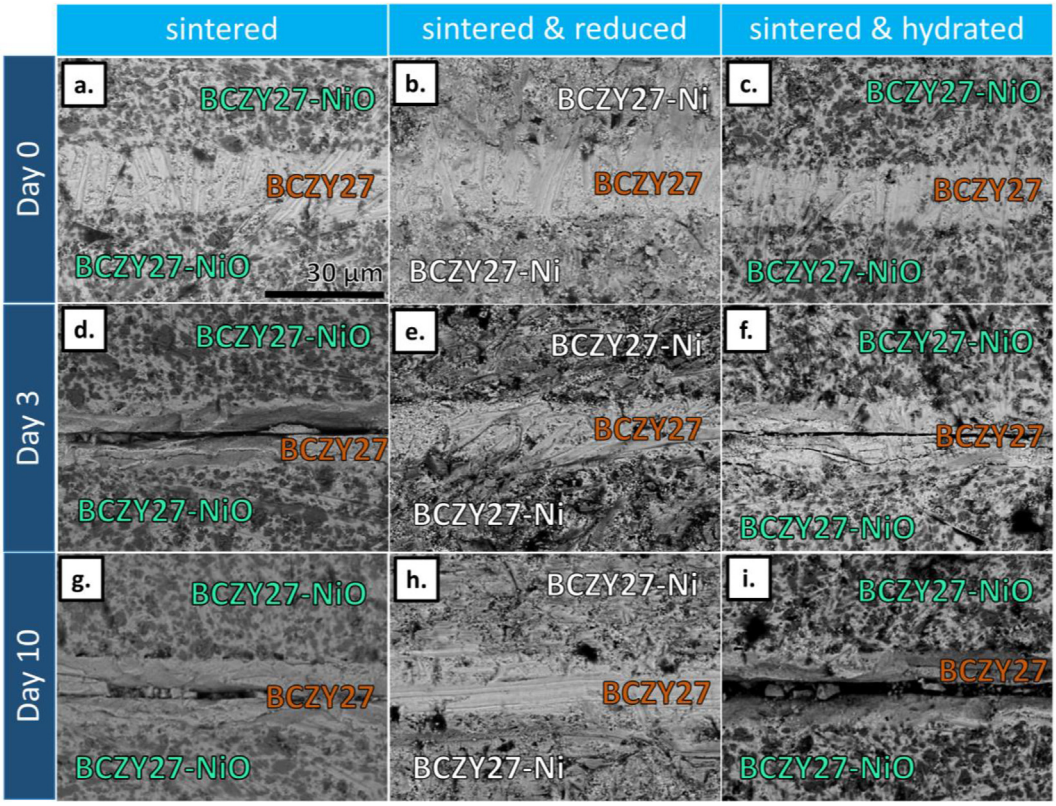

Fig. 2 – SEM images of fractured cross-section of PCC cells after: sintering (a., d., g.), sintering & heat treatment in reducing atmosphere (b., e., h), and sintering & heat treatment in hydrated atmosphere (c., f., i.). Images a., b. And c. Display the microstructure of PCC cells directly after the last heat treatment, while images d., e., f., and g., h., i., show the microstructure of the PCC cells after 3 and 10 days of storage in atmospheric conditions, respectively. All images are at the same scale.

Table 1 – Summary of SEM observations with regard to crack formation in the electrolyte.

1st crack appearance	sintered	sintered and reduced	sintered and hydrated
directly after last heat-treatment			
after **1 day** of storage in atmospheric conditions	1/3 cracked		
after **3 days** of storage in atmospheric conditions			
after **7 days** of storage in atmospheric conditions			
after **10 days** of storage in atmospheric conditions			
after **10 days** of storage under **vacuum**			1/3 cracked
after **120 days** of storage in atmospheric conditions			

approximately 40% lower than the one of 3YSZ–Ni. The observed difference can be explained in terms of the inherent different mechanical properties of 3YSZ and BCZY, and the microstructural differences between the two types of the supports (such as grain size and grain size distribution). For comparison, Sažinas and co-workers [48] have reported the fracture toughness of BCZY27 (i.e. without Ni), measured by Vickers micro-indentation technique, to be 1.65 (SD 0.11) MPa $m^{1/2,}$ whereas the fracture toughness of 3YSZ varies from 6.1 to 6.7 MPa $m^{1/2}$ depending on the fracture toughness testing methods used (double torsion and indentation, respectively) according to a study conducted by Chevalier et al. [49]. Moreover, it is worth mentioning that the fracture toughness values measured in the present work could be affected by the slow crack growth (SCG) phenomenon, as the measurements were carried in ambient air with a relatively slow displacement rate [50]. Further studies are thus required to comprehensively assess the susceptibility of BCZY27–Ni to slow crack growth, to understand the effects of microstructure and composition on the mechanical properties of the BCZY27–Ni composite, and ideally to enhance its mechanical properties towards that of the SoA zirconia-based supports.

Characterization of support and membrane layers by electrochemical impedance spectroscopy

EIS measurements were performed on the cells under open circuit voltage (OCV) condition in humidified (3% H_2O) 50% H_2/50% N_2 atmosphere in the temperature range of 650–800 °C and varying hydrogen partial pressure at 650 °C, as shown in Fig. 5a, and b. In the Nyquist plot, the intercept with the real axis at high frequency represents the ohmic resistance (R_S), and the difference between the high and low-frequency intercept represents the overall polarization resistance of the two identical electrodes (R_p). Two contributions are visible in the polarization resistance: the high-frequency one identified as R_H, and the low-frequency one referred to as R_L. In general, the higher frequency semicircle can be assigned to a charge transfer reaction (e.g. proton transfers between electrode and electrolyte), while the low-frequency semicircle can be ascribed to different elementary reactions on the surface,

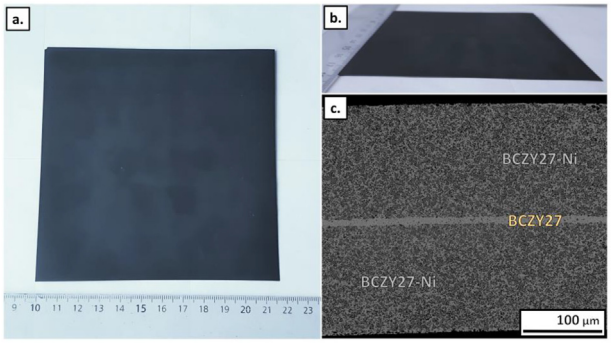

Fig. 3 – Pictures of up-scaled BCZY27–Ni | BCZY27 | BCZY27–Ni PCC cell (top view (a.) & side view (b.)), and corresponding polished cross-section of the cell (c.).

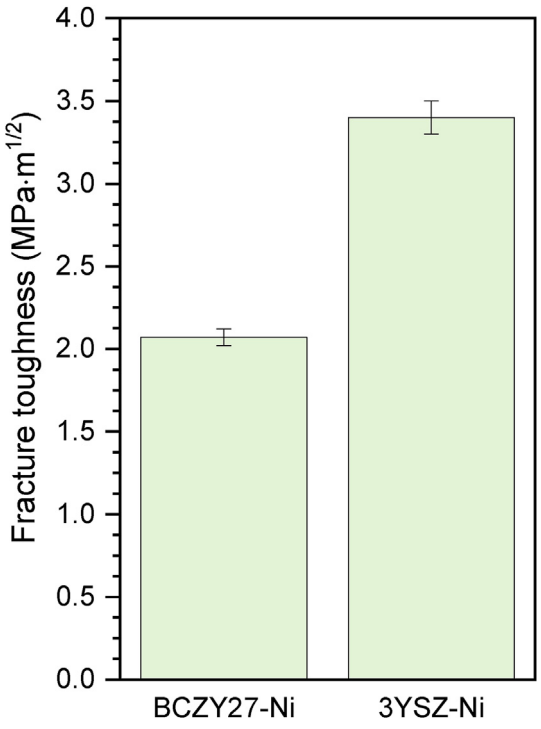

Fig. 4 – Room temperature fracture toughness of BCZY27–Ni support compared to 3YSZ–Ni [36], at porosity of ≈29%.

e.g. dissociation and adsorption of hydrogen or gas diffusion [51,52]. R_H is a thermally activated process and shows a small dependence on hydrogen partial pressure, as shown in Fig. 5a and b. Hence, R_H is likely associated with the charge transfer reaction [53]. R_L is characterized by a negligible thermal activation and shows attributes and is strongly affected by hydrogen partial pressure (Fig. 5a and b). R_L may be ascribed to hydrogen diffusion through the electrode. R_S is almost unaltered with the change of gas feeds, as expected for BCZY, which is a pure ionic conductor in a moist reducing atmosphere [24]. R_S increases with decreasing temperature (Fig. 5a). In the studied temperature range, the electrolyte material is partly dehydrated, and therefore the activation energy for proton transport cannot be calculated. One should note that the dehydration temperature varies significantly with the Zr/Ce ratio. Han et al. [54] reported an increase of the dehydration temperature in $BaCe_{0.8-x}Zr_xY_{0.2}O_{3-\delta}$ in 3.1% moist oxygen from 375 to 620 °C with increasing the cerium content from 0 to 0.8. The electrolyte conductivity, calculated based on the ohmic resistance, is plotted as a function of temperature in Fig. 5c. The values are within the range for BCZY prepared without the use of sintering aids [24]. According to the EIS analyses, the main limiting step of the electrode reaction process is the gas diffusion. It is particularly clear under low hydrogen content (20% pH_2) and at high temperatures (> 700 °C). In our future work, new samples will be prepared with a higher ratio of NiO (60 vol% instead of 50 vol %) in order to increase the porosity of the support (currently being 29%).

Indications regarding the electrochemical performance of our PCC cells can be found by comparing it with the performance of similar symmetrical cells from the literature. In this

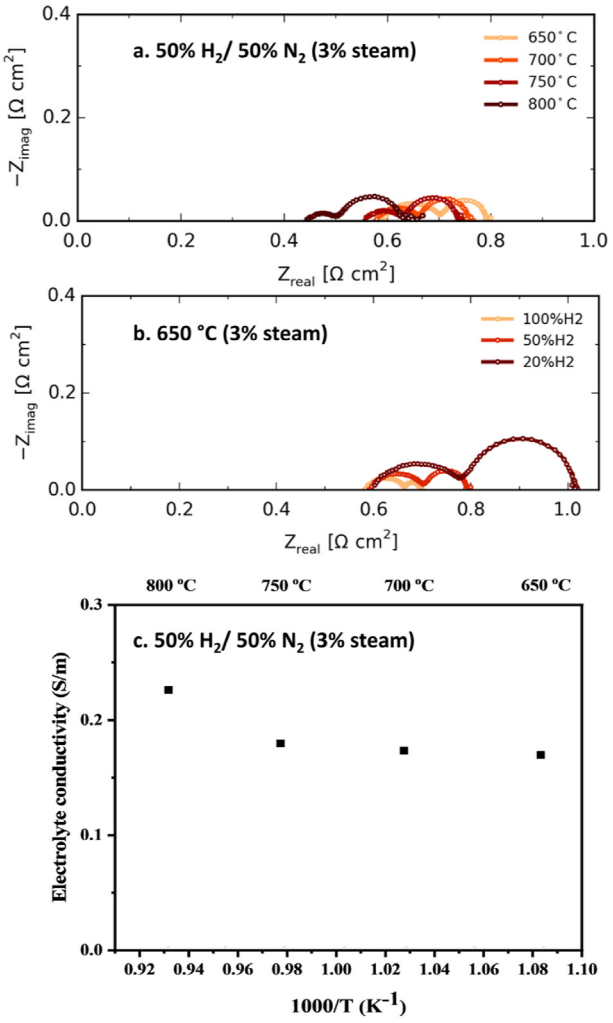

Fig. 5 – Nyquist plots of EIS data recorded on symmetrical cells at OCV and different temperatures (650–800 °C) under humidified (3% H_2O) 50% H_2/50%/N_2 (a.) and at 650 °C with varying hydrogen partial pressure (b.). Corresponding electrolyte conductivity under humidified (3% H_2O) 50% H_2/ 50% N_2 (c.).

work, BCZY27–Ni | BCZY27 | BCZY27–Ni protonic membranes exhibited R_s values of 0.59 and 0.44 Ω cm^2 at 650 and 800 °C (in 50% H_2/50% N_2, 3% H_2O). R_p values of 0.10 and 0.09 Ω cm^2 (per one electrode) were recorded in similar testing conditions. Comparable performances were recorded by other research groups with $BaZr_{0.8}Y_{0.2}O_{3-\delta}$ (BZY20), $BaCe_{0.7}Zr_{0.1}Y_{0.1}Yb_{0.1}O_{3-\delta}$ (BCZYYb), and $BaCe_{0.8}Zr_{0.1}Y_{0.1}O_{3-\delta}$ (BCZY811) symmetrical cells, as shown in Table 2.

Fig. 6 presents the durability measurement over 400 h on a symmetric cell tested at 650 °C in humidified (3% H_2O) 50% H_2/ 50% N_2 atmosphere, with negligible changes in the ohmic and polarization resistances. Therefore, this test highlights the good stability of the cell over 400 h. Based on these values, hydrogen fluxes of above 5 ml/cm^2/min can be expected, depending on the applied overpotential. Considering the large cell size and the possible compact design in a planar configuration, several applications related to hydrogen production can be envisioned. The extraction from pure hydrogen from diluted sources, steam methane (CH_4) reforming on a small scale, e.g. for hydrogen refueling stations, or the onboard production of hydrogen from liquid fuels in mobile applications (shipping, trucks, or fuel cell powered cars) have been identified as areas of interests, and will be pursued in the future.

In this study, BCZY27-based symmetrical protonic membranes were prepared and up-scaled to 135 cm^2. The cells were characterized microstructurally, mechanically and electrochemically. At first, the cells were microstructurally unstable due to hydration of the BCZY phase leading to chemical expansion of the electrolyte upon water uptake. However, this challenge was solved by reducing the cells soon after sintering, and large-size symmetrical cells could be prepared. The fracture toughness of BCZY27–Ni supports was assessed for the first time, corresponding to 2.07 (SD 0.05) MPa $m^{1/2}$. The electrochemical tests showed reasonable and stable performances in terms of ohmic and polarization resistances. In future works, the hydrogen permeation flux will be evaluated.

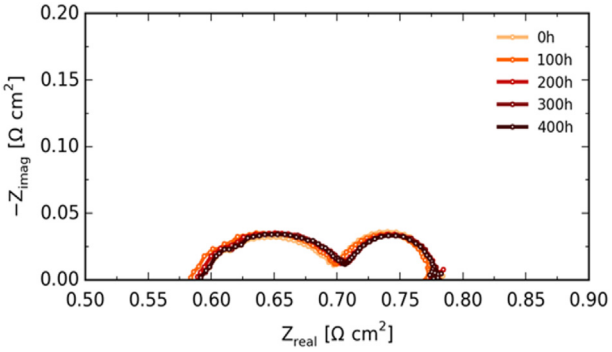

Fig. 6 – Nyquist plots recorded at 650 °C in humidified (3% H_2O) 50% H_2/50% N_2 atmosphere for 400 h.

Table 2 – Electrochemical performance of symmetrical PCG cells.

Electrolyte		Electrode	Gas composition	Temperature (°C)	R_s (Ω*cm^2)	R_p (Ω*cm^2)	Reference
Composition	Thickness (μm)						
BCZY27	13	BCZY27-Ni	50% H_2/50% N_2, 3% H_2O	650	0.59	0.10	This work
				800	0.44	0.09	
BZY20	20	BZY-Ni	100% H_2, 3% H_2O	600	0.57	0.14	[55]
BCZY811	40	BCZY811-Ni	20% H_2/80% Ar,	600	1.57	0.47	[56]
BCZYYb	60	BCZYYb	50% H_2/50% N_2, 3% H_2O	600	0.30	0.08	[57]

Conclusion

Symmetrical BCZY27–Ni | BCZY27 | BCZY27–Ni protonic membranes were manufactured by tape-casting, and co-sintering. Initially, the cells showed worrying microstructural degradation limiting their lifetime to only few days. Nevertheless, it was found that this challenge can be solved by performing a reducing heat treatment after sintering. As a result, the protonic cells appear to be microstructurally stable in the long-term (shelf live time >120 days) and were successfully up-scaled to 135 cm^2 (11.6 × 11.6 cm^2). Mechanical and electrochemical properties were investigated. The fracture toughness of the BCZY27–Ni cermet was studied for the first time and determined to be 2.07 (±0.05) MPa $m^{1/2}$. Impedance spectra were recorded on the symmetrical cells between 650 and 800 °C in humidified (3% H_2O) 50% H_2/50% N_2 atmosphere and at 650 °C, varying the hydrogen partial pressure. R_S was almost unaltered with the change of hydrogen partial pressure and decreased with increasing temperatures. Values of 0.59 and 0.44 Ω cm^2 were displayed at 650 and 800 °C, respectively (in 50% H_2/50% N_2, 3% H_2O). R_p was recorded at 0.10 and 0.09 Ω cm^2 (per one electrode) in similar testing conditions. A "long-term" stability test was performed over 400 h highlighting the stable electrochemical properties of the symmetrical membranes. Overall, this study reveals encouraging results for large-scale development of efficient PCC cells.

Author contributions

S.P. and R.K. conceived and designed the work. S.P. manufactured and up-scaled the cells. X.G. performed the microstructural stability study. P.K. carried out the mechanical tests and the corresponding data analyses. S.P. and X.G. performed the SEM analyses. Q.W. conducted the electrochemical tests and the corresponding data analyses. R.K., S.R. and M.C. supervised the research. S.P. wrote the manuscript. All authors reviewed and edited the manuscript.

Declaration of competing interest

The authors declare that they have no known competing financial interests or personal relationships that could have appeared to influence the work reported in this paper.

Acknowledgments

The financial support from the Independent Research Fund of Denmark through the "Hydrogen in demand – (H2Now)" project (grant number 9041-00334B) is gratefully acknowledged.

REFERENCES

[1] Mansilla C, Bourasseau C, Cany C, Guinot B, Le Duigou A, Lucchese P. Chapter 7: hydrogen applications: overview of the key economic issues and perspectives. In: Hydrog. Supply chain. Elsevier Ltd.; 2018. p. 271–92. https://doi.org/10.1016/b978-0-12-811197-0.00007-5.

[2] Jamal Y, Wyszynski ML. On-board generation of hydrogen-rich gaseous fuels-a review. Int J Hydrogen Energy 1994;19:557–72. https://doi.org/10.1016/0360-3199(94)90213-5.

[3] Cozzolino R, Tribioli L. On-board diesel autothermal reforming for PEM fuel cells: simulation and optimization. AIP Conf Proc 2015;1648. https://doi.org/10.1063/1.4912799.

[4] Tribioli L, Cozzolino R, Chiappini D. Technical assessment of different operating conditions of an on-board autothermal reformer for fuel cell vehicles. Energies 2017;10. https://doi.org/10.3390/en10070839.

[5] Dailly J, Marrony M. BCY-based proton conducting ceramic cell: 1000 h of long term testing in fuel cell application. J Power Sources 2013;240:323–7. https://doi.org/10.1016/j.jpowsour.2013.04.028.

[6] Dailly J, Ancelin M, Marrony M. Long term testing of BCZY-based protonic ceramic fuel cell PCFC: micro-generation profile and reversible production of hydrogen and electricity. Solid State Ionics 2017;306:69–75. https://doi.org/10.1016/j.ssi.2017.03.002.

[7] Bae K, Noh HS, Jang DY, Hong J, Kim H, Yoon KJ, Lee JH, Kim BK, Shim JH, Son JW. High-performance thin-film protonic ceramic fuel cells fabricated on anode supports with a non-proton-conducting ceramic matrix. J Mater Chem A 2016;4:6395–404. https://doi.org/10.1039/c5ta10670b.

[8] Vasileiou E, Kyriakou V, Garagounis I, Vourros A, Stoukides M. Ammonia synthesis at atmospheric pressure in a BaCe0.2Zr0.7Y0.1O2.9 solid electrolyte cell. Solid State Ionics 2015;275:110–6. https://doi.org/10.1016/j.ssi.2015.01.002.

[9] Morejudo SH, Zanón R, Escolástico S, Yuste-Tirados I, Malerød-Fjeld H, Vestre PK, Coors WG, Martínez A, Norby T, Serra JM, Kjølseth C. Direct conversion of methane to aromatics in a catalytic co-ionic membrane reactor. Science 2016;353:563–6. https://doi.org/10.1126/science.aag0274.

[10] Ding D, Zhang Y, Wu W, Chen D, Liu M, He T. A novel low-thermal-budget approach for the co-production of ethylene and hydrogen via the electrochemical non-oxidative deprotonation of ethane. Energy Environ Sci 2018;11:1710–6. https://doi.org/10.1039/c8ee00645h.

[11] Malerød-Fjeld H, Clark D, Yuste-Tirados I, Zanón R, Catalán-Martinez D, Beeaff D, Morejudo SH, Vestre PK, Norby T, Haugsrud R, Serra JM, Kjølseth C. Thermo-electrochemical production of compressed hydrogen from methane with near-zero energy loss. Nat Energy 2017;2:923–31. https://doi.org/10.1038/s41560-017-0029-4.

[12] Dubois A, Ricote S, Braun RJ. Benchmarking the expected stack manufacturing cost of next generation, intermediate-temperature protonic ceramic fuel cells with solid oxide fuel cell technology. J Power Sources 2017;369:65–77. https://doi.org/10.1016/j.jpowsour.2017.09.024.

[13] Duan C, Tong J, Shang M, Nikodemski S, Sanders M, Ricote S, Almansoori A, O'Hayre R. Readily processed protonic ceramic fuel cells with high performance at low temperatures. Science 2015;349:1321–6. https://doi.org/10.1126/science.aab3987.

[14] Duan C, Kee RJ, Zhu H, Karakaya C, Chen Y, Ricote S, Jarry A, Crumlin EJ, Hook D, Braun R, Sullivan NP, O'Hayre R. Highly durable, coking and sulfur tolerant, fuel-flexible protonic ceramic fuel cells. Nature 2018;557:217–22. https://doi.org/10.1038/s41586-018-0082-6.

[15] Choi S, Kucharczyk CJ, Liang Y, Zhang X, Takeuchi I, Il Ji H, Haile SM. Exceptional power density and stability at intermediate temperatures in protonic ceramic fuel cells. Nat Energy 2018;3:202–10. https://doi.org/10.1038/s41560-017-0085-9.

[16] Bae K, Jang DY, Choi HJ, Kim D, Hong J, Kim BK, Lee JH, Son JW, Shim JH. Demonstrating the potential of yttrium-doped barium zirconate electrolyte for high-performance fuel cells. Nat Commun 2017;8:1–9. https://doi.org/10.1038/ncomms14553.
[17] Fabbri E, Bi L, Pergolesi D, Traversa E. Towards the next generation of solid oxide fuel cells operating below 600 °c with chemically stable proton-conducting electrolytes. Adv Mater 2012;24:195–208. https://doi.org/10.1002/adma.201103102.
[18] Kreuer KD. Proton-conducting oxides. Annu Rev Mater Res 2003;33:333–59. https://doi.org/10.1146/annurev.matsci.33.022802.091825.
[19] Shirpour M, Merkle R, Maier J. Evidence for space charge effects in Y-doped BaZrO3 from reduction experiments. Solid State Ionics 2012;216:1–5. https://doi.org/10.1016/j.ssi.2011.09.006.
[20] Katahira K, Kohchi Y, Shimura T, Iwahara H. Protonic conduction in Zr-substituted BaCeO3. Solid State Ionics 2000;138:91–8. https://doi.org/10.1016/S0167-2738(00)00777-3.
[21] Duan C, Kee R, Zhu H, Sullivan N, Zhu L, Bian L, Jennings D, O'Hayre R. Highly efficient reversible protonic ceramic electrochemical cells for power generation and fuel production. Nat Energy 2019;4:230–40. https://doi.org/10.1038/s41560-019-0333-2.
[22] Deibert W, Ivanova ME, Baumann S, Guillon O, Meulenberg WA. Ion-conducting ceramic membrane reactors for high-temperature applications. J Membr Sci 2017;543:79–97. https://doi.org/10.1016/j.memsci.2017.08.016.
[23] Kyriakou V, Garagounis I, Vourros A, Vasileiou E, Manerbino A, Coors WG, Stoukides M. Methane steam reforming at low temperatures in a BaZr0.7Ce0.2Y0.1O2.9 proton conducting membrane reactor. Appl Catal B Environ 2016;186:1–9. https://doi.org/10.1016/j.apcatb.2015.12.039.
[24] Ricote S, Bonanos N, Caboche G. Water vapour solubility and conductivity study of the proton conductor BaCe(0.9 - x) ZrxY0.1O(3 - δ). Solid State Ionics 2009;180:990–7. https://doi.org/10.1016/j.ssi.2009.03.016.
[25] Babilo P, Haile SM. Enhanced sintering of yttrium-doped barium zirconate by addition of ZnO. J Am Ceram Soc 2005;88:2362–8. https://doi.org/10.1111/j.1551-2916.2005.00449.x.
[26] Tao S, Irvine JTS. A stable, easily sintered proton-conducting oxide electrolyte for moderate-temperature fuel cells and electrolyzers. Adv Mater 2006;18:1581–4. https://doi.org/10.1002/adma.200502098.
[27] Ricote S, Bonanos N. Enhanced sintering and conductivity study of cobalt or nickel doped solid solution of barium cerate and zirconate. Solid State Ionics 2010;181:694–700. https://doi.org/10.1016/j.ssi.2010.04.007.
[28] Azimova MA, McIntosh S. Transport properties and stability of cobalt doped proton conducting oxides. Solid State Ionics 2009;180:160–7. https://doi.org/10.1016/j.ssi.2008.12.013.
[29] Fang S, Bi L, Yang C, Yan L, Chen C, Liu W. H2S poisoning and regeneration of Ni-BaZr0.1Ce0.7Y0.2O3-δ at intermediate temperature. J Alloys Compd 2009;475:935–9. https://doi.org/10.1016/j.jallcom.2008.08.070.
[30] Fang S, Bi L, Wu X, Gao H, Chen C, Liu W. Chemical stability and hydrogen permeation performance of Ni-BaZr0.1Ce0.7Y0.2O3-δ in an H2S-containing atmosphere. J Power Sources 2008;183:126–32. https://doi.org/10.1016/j.jpowsour.2008.05.015.
[31] Zuo C, Dorris SE, Balachandran U, Liu M. Effect of Zr-doping on the chemical stability and hydrogen permeation of the Ni-BaCe0.8y 0.2O3-α mixed protonic-electronic conductor. Chem Mater 2006;18:4647–50. https://doi.org/10.1021/cm0518224.
[32] Zuo C, Lee TH, Song SJ, Chen L, Dorris SE, Balachandran U, Liu M. Hydrogen permeation and chemical stability of cermet [Ni-Ba(Zr0.8-xCexy0.2)O3] membranes. Electrochem Solid-State Lett 2005;8:J35–7. https://doi.org/10.1149/1.2081807.
[33] Zuo C, Lee TH, Dorris SE, Balachandran U, Liu M. Composite Ni-Ba(Zr0.1Ce0.7Y0.2)O3 membrane for hydrogen separation. J Power Sources 2006;159:1291–5. https://doi.org/10.1016/j.jpowsour.2005.12.042.
[34] Mistler RE, Twiname ER. Tape Casting: theory and practice. Westerville, Ohio: The American Ceramic Society; 2000.
[35] Pirou S. Development of dual-phase oxygen transport membranes for carbon capture processes. Technical University of Denmark; 2017.
[36] Khajavi P, Hendriksen PV, Chevalier J, Gremillard L, Frandsen HL. Improving the fracture toughness of stabilized zirconia-based solid oxide cells fuel electrode supports: effects of type and concentration of stabilizer(s). J Eur Ceram Soc 2020;40:5670–82. https://doi.org/10.1016/j.jeurceramsoc.2020.05.042.
[37] Jensen SH, Hauch A, Hendriksen PV, Mogensen M. Advanced test method of solid oxide cells in a plug-flow setup. J Electrochem Soc 2009;156:B757. https://doi.org/10.1149/1.3116247.
[38] Nielsen J, Hjelm J. Impedance of SOFC electrodes : a review and a comprehensive case study on the impedance of LSM:YSZ cathodes. Electrochim Acta 2014;115:31–45. https://doi.org/10.1016/j.electacta.2013.10.053.
[39] Ramos T, Thydén K, Mogensen M. Electrochemical characterization of Ni/(Sc)YSZ electrodes. ECS Trans 2010;28:123–39.
[40] Graves C. RAVDAV data analysis software. 2011. p. 1–43.
[41] Løken A, Ricote S, Wachowski S. Thermal and chemical expansion in proton ceramic electrolytes and compatible electrodes. Crystals 2018:8. https://doi.org/10.3390/cryst8090365.
[42] Khajavi P, Frandsen HL, Gremillard L, Chevalier J, Hendriksen PV. Strength and hydrothermal stability of NiO–stabilized zirconia solid oxide cells fuel electrode supports. J Eur Ceram Soc 2021;41:4206–16. https://doi.org/10.1016/j.jeurceramsoc.2021.01.052.
[43] Escribano JA, García-Fayos J, Serra JM. Shaping of 3YSZ porous substrates for oxygen separation membranes. J Eur Ceram Soc 2017;37:5223–31. https://doi.org/10.1016/j.jeurceramsoc.2017.05.032.
[44] Pirou S, Gurauskis J, Gil V, Søgaard M, Hendriksen PV, Kaiser A, Ovtar S, Kiebach R. Oxygen permeation flux through 10Sc1YSZ-MnCo2O4 asymmetric membranes prepared by two-step sintering, Fuel Process. Technol 2016;152:192–9. https://doi.org/10.1016/j.fuproc.2016.06.019.
[45] Pirou S, Bermudez JM, Hendriksen PV, Kaiser A, Reina TR, Millan M, Kiebach R. Stability and performance of robust dual-phase (ZrO2)0.89(Y2O3)0.01(Sc2O3)0.10-Al0.02Zn0.98O1.01 oxygen transport membranes. J Membr Sci 2017;543:18–27. https://doi.org/10.1016/j.memsci.2017.08.044.
[46] Hauch A, Küngas R, Blennow P, Hansen AB, Hansen JB, Mathiesen BV, Mogensen MB. Recent advances in solid oxide cell technology for electrolysis. Science 2020:370. https://doi.org/10.1126/science.aba6118.
[47] Chen X, Ni W, Du X, Sun Z, Zhu T, Zhong Q, Han M. Electrochemical property of multi-layer anode supported solid oxide fuel cell fabricated through sequential tape-casting and co-firing. J Mater Sci Technol 2019;35:695–701. https://doi.org/10.1016/j.jmst.2018.10.015.

[48] Sažinas R, Einarsrud MA, Grande T. Toughening of Y-doped BaZrO3 proton conducting electrolytes by hydration. J Mater Chem A 2017;5:5846–57. https://doi.org/10.1039/c6ta11022c.
[49] Chevalier J, Olagnon C, Fantozzi G. Subcritical crack propagation in 3Y-TZP ceramics: static and cyclic fatigue. J Am Ceram Soc 1999;82:3129–38. https://doi.org/10.1111/j.1151-2916.1999.tb02213.x.
[50] Khajavi P, Chevalier J, Vang P, Tavacoli JW, Gremillard L, Lund Frandsen H. Double Torsion testing of thin porous zirconia supports for energy applications : toughness and slow crack growth assessment. J Eur Ceram Soc 2020;40:3191–9. https://doi.org/10.1016/j.jeurceramsoc.2020.02.019.
[51] Dailly J, Mauvy F, Marrony M, Pouchard M, Grenier JC. Electrochemical properties of perovskite and A2MO 4-type oxides used as cathodes in protonic ceramic half cells. J Solid State Electrochem 2011;15:245–51. https://doi.org/10.1007/s10008-010-1188-4.
[52] Bausá N, Solís C, Strandbakke R, Serra JM. Development of composite steam electrodes for electrolyzers based on barium zirconate. Solid State Ionics 2017;306:62–8. https://doi.org/10.1016/j.ssi.2017.03.020.
[53] Ricote S, Bonanos N, Rørvik PM, Haavik C. Microstructure and performance of La 0.58Sr 0.4Co 0.2Fe 0.8O 3-δ cathodes deposited on BaCe 0.2Zr 0.7Y 0.1O 3-δ by infiltration and spray pyrolysis. J Power Sources 2012;209:172–9. https://doi.org/10.1016/j.jpowsour.2012.02.090.
[54] Han D, Liu X, Bjørheim TS, Uda T. Yttrium-doped barium zirconate-cerate solid solution as proton conducting electrolyte: why higher cerium concentration leads to better performance for fuel cells and electrolysis cells. Adv Energy Mater 2021;11. https://doi.org/10.1002/aenm.202003149.
[55] Onishi T, Han D, Noda Y, Hatada N, Majima M, Uda T. Evaluation of performance and durability of Ni-BZY cermet electrodes with BZY electrolyte. Solid State Ionics 2018;317:127–35.
[56] Mao V. Novel mixed protonic-electronic materials : development of selective membranes devoted for hydrogen separation. Montpellier University; 2016.
[57] Pers P, Mao V, Taillades M, Taillades G. Electrochemical behavior and performances of Ni-BaZr0·1Ce0·7Y0.1Yb0.1O3–δ cermet anodes for protonic ceramic fuel cell. Int J Hydrogen Energy 2018;43:2402–9. https://doi.org/10.1016/j.ijhydene.2017.12.024.